Supporting Information

Hydride Attack on a Coordinated Ferric Nitrosyl: Experimental and DFT Evidence for the Formation of a Heme Model-HNO Derivative

Erwin G. Abucayon,† Rahul L. Khade,‡ Douglas R. Powell,† Yong Zhang,*,‡ George B. Richter-Addo,*,†

Contents:

1. Experimental
2. Figure S1. Difference spectra (product minus reactant) showing the new NO bands for (OEP)Fe(HNO)(5-MeIm) and the $H^{15}NO$ derivative
3. Figure S2. ^1H NMR spectra of (a) the precursor [(OEP)Fe(NO)(5-MeIm)]OTf, and (b) the product mixture after addition of hydride.
4. Figure S3. ^1H NMR spectroscopic detection of the H_2 (in $CDCl_3$) by-product from the decomposition of (OEP)Fe(HNO)(5-MeIm). (A) Spectrum of the blank $CDCl_3$ solvent. (B) Spectrum of the reaction headspace. (C) Spectrum of the authentic H_2/N_2 mixture
5. Figure S4. FTIR monitoring of the thermal decomposition of (a) (OEP)Fe(HNO)(5-MeIm) (υ_{NO} 1383 cm^{-1}) to (OEP)Fe(NO) (υ_{NO} 1668 cm^{-1}), and (b) (OEP)Fe($H^{15}NO$)(5-MeIm) (υ_{NO} 1360 cm^{-1}) to (OEP)Fe(^{15}NO) (υ_{NO} 1636 cm^{-1})
6. Figure S5. Molecular structure of the cation
7. Figure S6. Crystal packing diagram
8. X-ray experimental
9. Table S1. Crystal data and structure refinement for [(OEP)Fe(NO)(5-MeIm)]OTf.0.5CH_2Cl_2
10. Table S2. Atomic coordinates and equivalent isotropic displacement parameters
11. Table S3. Bond lengths and angles
12. Table S4. Anisotropic displacement parameters
13. Table S5. Hydrogen coordinates and isotropic displacement parameters
14. Table S6. Torsion angles
15. Table S7. Hydrogen bonds
16. Computational details
17. Scheme S1. DFT-calculated N- and O-pathways for hydride addition to the $[(P)Fe(NO)(5\text{-MeIm})]^+$ cation.
18. Figure S7. Optimized structures of (A) Fe^{II}(Por)(5-MeIm)(NOH_{up}) and (B) Fe^{II}(Por)(5-MeIm)(NOH_{down})
19. Table S8. Relative Energies of All Species in the N- and O-pathways from mPW1PW91

20. Table S9. Relative Energies of All Species in the N- and O-pathways from mPWVWN calculations
21. Table S10. Relative Energies of All Species in the N- and O-pathways from B3LYP-D3 calculations
22. Table S11. Key Geometry Parameters from mPW1PW91 Calculations
23. Table S12. NPA Charges from mPW1PW91 Calculations

Experimental

General: The reactions were performed anaerobically using nitrogen as an inert gas. Air-sensitive samples and reagents were handled inside the glove box and all reactions were done in standard Schlenk glassware. Solvents used in the reactions were collected under nitrogen from a Pure Solv 400-5-MD Solvent Purification System (Innovative Technology) or distilled from appropriate drying agents under an atmosphere of nitrogen gas. Nitric oxide (NO) gas was passed through potassium hydroxide column, then through a cold trap prior to its contact with the precursor solution to avoid the introduction of NO_x impurities. ^{15}NO (Icon Isotope Inc., 99% ^{15}N) was used as received without further purification. FT-IR spectra for compound characterization were recorded on a Bruker Tensor 27 spectrometer. ^1H NMR spectra were collected on a 400 MHz Varian NMR instrument at -20°C. ESI mass spectra were obtained in a high resolution Micromass Q-TOF mass spectrometer. Elemental analyses were performed by Atlantic Microlab Inc., Norcross, GA, USA.

Preparation of [(OEP)Fe(NO)(5-MeIm)]OTf. To a CH_2Cl_2 (5 mL) solution of (OEP)Fe(OTf)[1-2] (16.8 mg, 0.023 mmol) was added 4/5-methylimidazole (2.1 mg, 0.025 mmol) followed by NO gas, in a similar manner used to prepare other crystalline $[(por)Fe(NO)(N\text{-ligand})]^+$ complexes.[4] X-ray quality crystals of the product [(OEP)Fe(NO)(5-MeIm)]OTf (10.1 mg, 52% isolated yield based on the (OEP)Fe(OTf) precursor) were obtained from its CH_2Cl_2/*n*-hexane solution. Anal. Calcd for $C_{41}H_5F_3FeN_7O_4S{\cdot}0.5CH_2Cl_2$: C, 55.86; H, 5.76; N, 10.99; S, 3.59. Found: C, 56.84; H, 5.98; N, 10.93; S, 3.40. Solution IR (CH_2Cl_2) of (OEP)Fe(NO)(5-MeIm)OTf: υ_{NO} =1910 cm^{-1} (υ_{15NO} = 1874 cm^{-1}). IR (KBr): υ_{NO} =1895 cm^{-1}. Characteristic bands of an uncoordinated triflate anion:[2] υ_{as} (SO_3) =1295 cm^{-1}, υ_s (CF_3) =1225 cm^{-1}, υ_s(SO_3) = 1022 cm^{-1}.[3] UV-Vis (CH_2Cl_2): λ, 411, 526, 558 nm.[4] ^1H NMR ($CDCl_3$, -20 °C, 400 MHz; ppm): δ = 10.19 (*s*, 4H, Methine-H), 9.25 (*s*, 1H, 5-MeIm N-H), 7.26 (*s*, $CHCl_3$), 5.32 (*s*, CH_2Cl_2), 4.13 (*overlapping q*, 16H, ethyl-CH_2), 1.97(*t*, $J_{H\text{-}H}$ = 7.6 Hz, 24H, ethyl-CH_3), 1.23 (*br*, *n*-hexane), 0.86 (*t*, $J_{H\text{-}H}$ = 8.0 Hz, *n*-hexane), 0.45 (*s*, 3H, 5-MeIm-CH_3), 0.22 (*s*, 1H, 5-MeIm), -0.77 (*s*, 1H, 5-MeIm). High resolution ESI mass spectrum of the [(OEP)Fe(NO)(5-MeIm)]OTf: positive (+) mode, *m/z* of $[(OEP)Fe(5\text{-}MeIm]^+$ = 670.3447, *m/z* of $[(OEP)Fe]^+$ = 588.2916; and negative (-) mode, *m/z* of $[OSO_2CF_3]^-$ = 148.9520

Preparation of (OEP)Fe(HNO)(5-MeIm). To a $CDCl_3$ (1.5 mL) solution of [(OEP)Fe(NO)(5-MeIm)]OTf (9.5 mg, 0.011 mmol; IR υ_{NO} =1910 cm^{-1} (υ_{15NO} =1874 cm^{-1})) in a J. Young NMR tube at -20 °C was added a $CDCl_3$ (0.2 mL) solution of $[NBu_4]BH_4$ (4.5 mg, 0.017 mmol). The ^1H NMR spectra were recorded immediately. The characteristic NO stretching frequency of the (OEP)Fe(HNO)(5-MeIm) complex was obtained from a separate reaction in $CHCl_3$ at -20°C (IR υ_{NO}=1383 cm^{-1}, υ_{15NO}=1360 cm^{-1}); Figure S1.

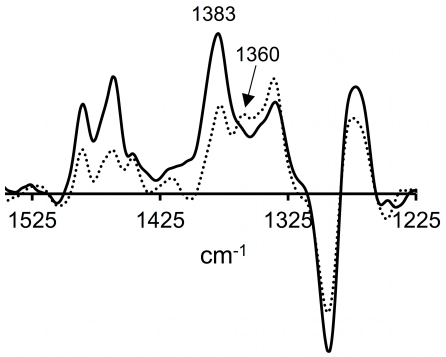

Figure S1. Difference spectra (product minus reactant) showing the new NO bands for (OEP)Fe(HNO)(5-MeIm) (solid line; 1383 cm^{-1}) and the $H^{15}NO$ derivative (dashed line; 1360 cm^{-1}).

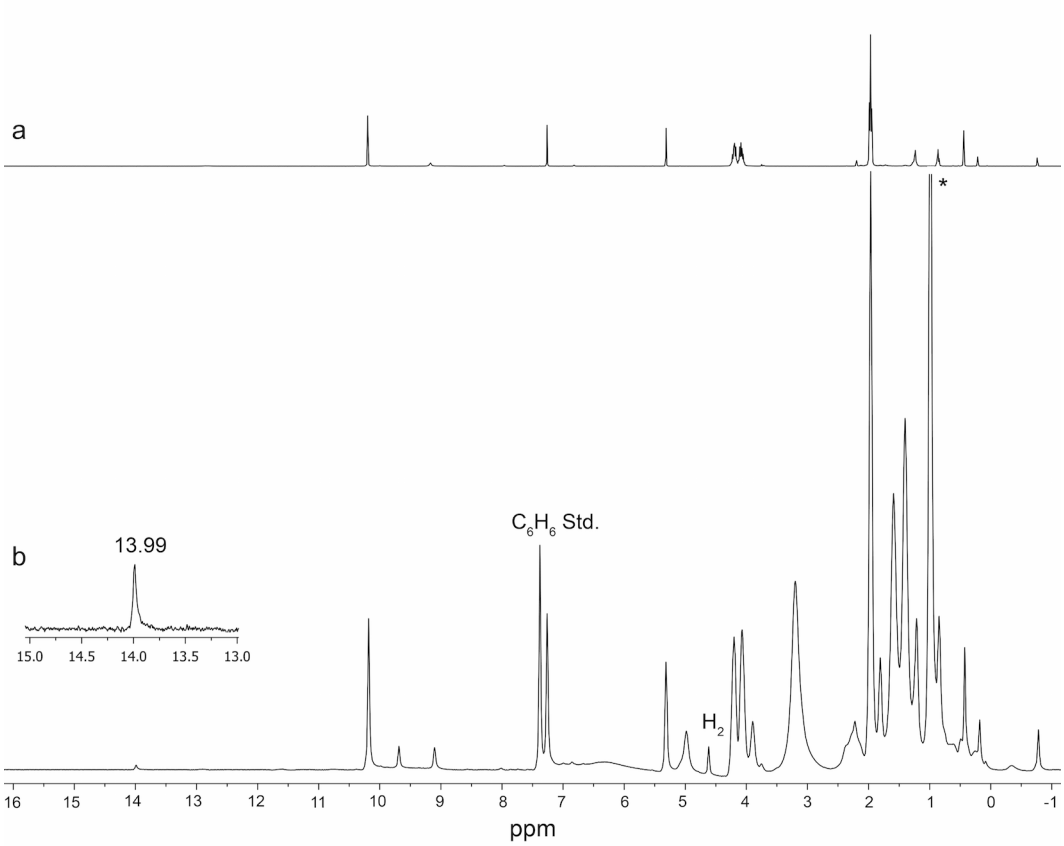

Figure S2. ^1H NMR spectra of (a) the precursor [(OEP)Fe(NO)(5-MeIm)]OTf in $CDCl_3$ (-20 °C, 400 MHz; ppm): δ = 10.19 (*s*, 4H, methine-H), 9.25 (*s*, 1H, 5-MeIm N-H), 7.26 (*s*, $CHCl_3$), 5.32 (*s*, CH_2Cl_2), 4.13 (*overlapping q*, 16H, ethyl-CH_2), 1.97(*t*, J_{H-H} = 7.6 Hz, 24H, ethyl-CH_3), 1.23 (*br*, *n*-hexane), 0.86 (*t*, J_{H-H} = 8.0 Hz, *n*-hexane), 0.45 (*s*, 3H, 5-MeIm-CH_3), 0.22 (*s*, 1H, 5-MeIm), -0.77 (*s*, 1H, 5-MeIm), and (b) the product mixture after addition of hydride. The broadness of the peaks are likely due to the presence of the paramagnetic (OEP)Fe(NO) decomposition product; the peak at 4.62 ppm is assigned to H_2 (see Figure S3). The HNO signal (~11% yield) was integrated against a C_6H_6 internal standard.

Reaction of (OEP)Fe(HNO)(5-MeIm) with PPh_3. To the *in situ* generated (OEP)Fe(HNO)(5-MeIm) in $CHCl_3$ at -20 °C was added excess PPh_3 (solid), and the resulting mixture was stirred for 5 min at this temperature. The reacting solution was warmed slowly to room temperature and stirred for another 30 min. High resolution ESI mass spectra of the reaction mixture: *m/z* of $[HN{=}PPh_3]^+$ = 278.1101 (expected 278.1099), *m/z* of $[O{=}PPh_3]^+$ = 279.0937 (expected 279.0939).

Detection of H_2 from the decomposition of (OEP)Fe(HNO)(5-MeIm) to (OEP)Fe(NO). The headspace gas of the reaction mixture to generate (OEP)Fe(HNO)(5-MeIm) was collected after warming the mixture to room temperature. The headspace gas was then injected into $CDCl_3$ and the ^1H NMR spectrum was recorded. ^1H NMR data: 7.26 (*s*, $CHCl_3$), 4.62 (*s*, dissolved H_2 gas).[5] These data matched an authentic commercial sample of 5% H_2/N_2 (see Figure S3).

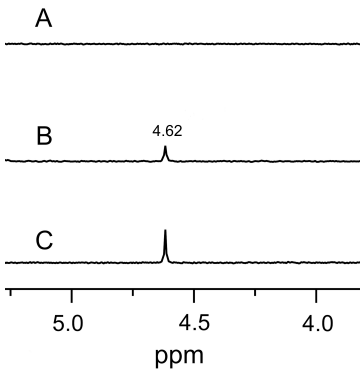

Figure S3. ^1H NMR spectroscopic detection of the H_2 (in $CDCl_3$) by-product from the decomposition of (OEP)Fe(HNO)(5-MeIm). (A) Spectrum of the blank $CDCl_3$ solvent. (B) Spectrum of the reaction headspace. (C) Spectrum of the authentic H_2/N_2 mixture.

The identity of H_2 was further confirmed by gas chromatography (GC), by injection of 30 μL of the headspace gas using an air-tight syringe into a Shimadzu gas chromatograph (GC-8A) equipped with thermal conductivity detector (TCD) and fitted with 50/80 Porapak Q (2m x 1/8 in) column. GC conditions: Tank pressure: 22 psi, inj/det temp.: 110°C, column temp.: 100°C, and current: 100 mA. The GC instrument was pre-calibrated using two $H_2/CO_2/N_2$ mixtures of known compositions.

IR monitoring of the reaction also showed formation of the known five-coordinate (OEP)Fe(NO) (Figure S4).

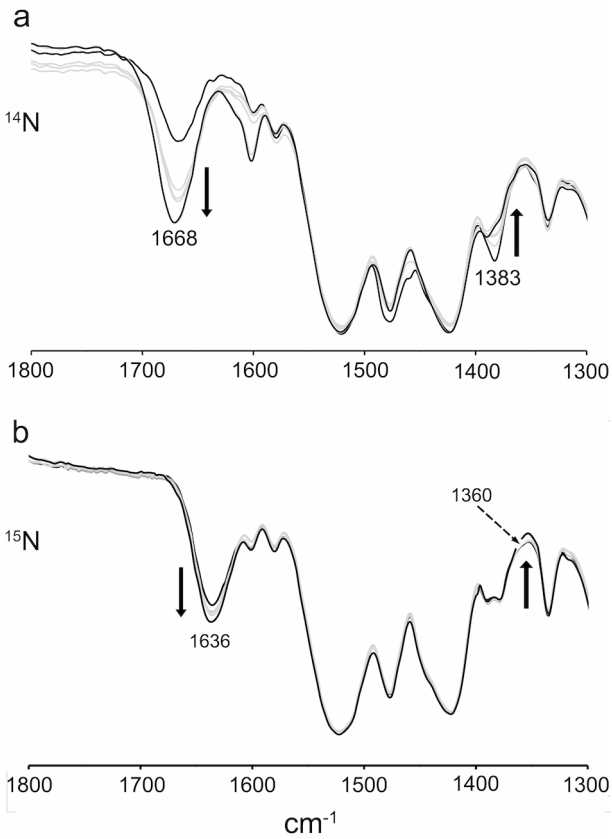

Figure S4. FTIR monitoring of the thermal decomposition of (a) (OEP)Fe(HNO)(5-MeIm) (υ_{NO} 1383 cm^{-1}) to (OEP)Fe(NO) (υ_{NO} 1668 cm^{-1}), and (b) (OEP)Fe(H^{15}NO)(5-MeIm) (υ_{NO} 1360 cm^{-1}) to (OEP)Fe(^{15}NO) (υ_{NO} 1636 cm^{-1}).

References

1. Ogoshi, H., Watanabe, E., and Yoshida, Z. *Chem. Lett*. **1973**, 989-992.
2. Dolphin, D. H., Sams, J. R., and Tsin, T. B. *Inorg. Chem*. **1977**, 16, 711-713.
3. D. H. Johnston and D. F. Shriver. *Inorg. Chem*. **1993**, 32, 1045.
4. Ellison, M. K. and Scheidt, R. *J. Am. Chem. Soc*. **1999**, 121, 5210-5219.
5. Fulmer, G. R., Miller, A. J. M., Sherden, N. H., Gottlied, H. E., Nudelman, A., Stoltz, B. M., Bercaw, J. E., and Goldberg, K. I. *Organometallics* **2010**, 29, 2176-2179.

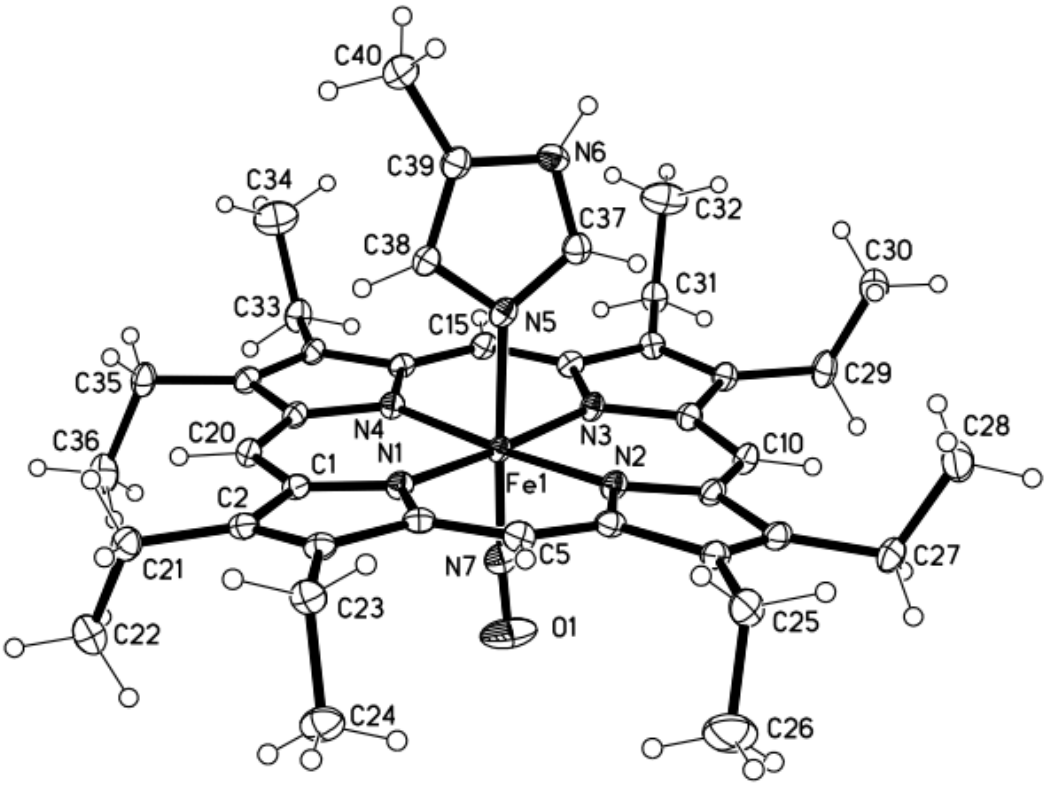

Figure S5. Molecular structure of the cation.

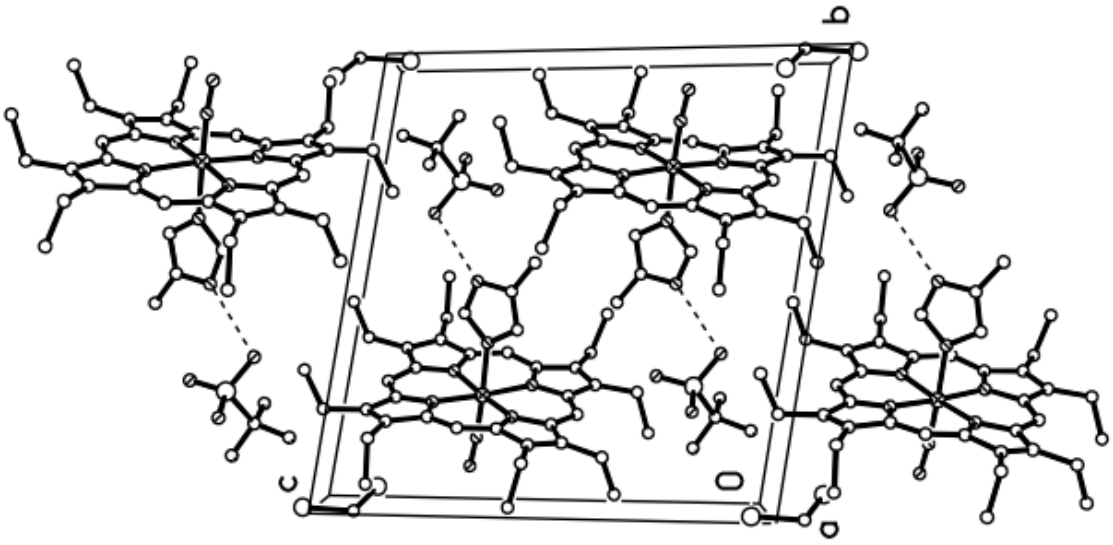

Figure S6. Crystal packing diagram.

Comment

The solvent molecule was located near to an inversion center; thus, the occupancy of this molecule can be at most ½. Because of the proximity of the inversion center, restraints on the positional and displacement parameters of the solvent atoms were required. The displacement ellipsoids were drawn at the 50% probability level.

Experimental

A red, block-shaped crystal of dimensions 0.550 x 0.520 x 0.380 mm was selected for structural analysis. Intensity data for this compound were collected using a diffractometer with a Bruker APEX ccd area detector[1] and graphite-monochromated Mo Kα radiation (λ = 0.71073 Å). The sample was cooled to 100(2) K. Cell parameters were determined from a non-linear least squares fit of 9887 peaks in the range $2.40 < \theta < 27.47°$. A total of 36273 data were measured in the range $1.319 < \theta < 27.497°$ using ϕ and ω oscillation frames. The data were corrected for absorption by the empirical method[2] giving minimum and maximum transmission factors of 0.757 and 0.822. The data were merged to form a set of 9360 independent data with R(int) = 0.0481 and a coverage of 99.1%.

The triclinic space group $P\bar{1}$ was determined by statistical tests and verified by subsequent refinement. The structure was solved by direct methods and refined by full-matrix least-squares methods on F^2.[3] The positions of hydrogens bonded to carbons were initially determined by geometry and were refined using a riding model. The hydrogen bonded to N6 was located on a difference map, and its position was refined independently. Non-hydrogen atoms were refined with anisotropic displacement parameters. Hydrogen atom displacement parameters were set to 1.2 (1.5 for methyl) times the isotropic equivalent displacement parameters of the bonded atoms. A total of 545 parameters were refined against 10 restraints and 9360 data to give $wR(F^2) = 0.1073$ and S = 0.982 for weights of $w = 1/[\sigma^2 (F^2) + (0.0500 P)^2 + 2.0000 P]$, where $P = [F_o^2 + 2F_c^2] / 3$. The final R(F) was 0.0383 for the 7918 observed, [$F > 4\sigma(F)$], data. The largest shift/s.u. was 0.001 in the final refinement cycle. The final difference map had maxima and minima of 0.820 and -0.461 e/Å^3, respectively.

Acknowledgment

The authors thank the National Science Foundation (grant CHE-0130835) and the University of Oklahoma for funds to purchase of the X-ray instrument and computers. This structure was determined by Douglas R. Powell.

References

1. (a) Data Collection: APEX2 (2007) Bruker AXS Inc., Madison, Wisconsin, USA. (b) Data Reduction: SAINT (2007) Bruker AXS Inc., Madison, Wisconsin, USA.
2. SADABS (2002) Bruker AXS Inc., Madison, Wisconsin, USA.
3. (a) G. M. Sheldrick. *Acta Cryst.,* **2015**, *C71*, 3-8. (b) G. M. Sheldrick. *Acta Cryst.,* **2015**, *A71*, 3-8.

Deposition of the crystal structure with the CCDC

CCDC 1436952 contains the supplementary crystallographic data. These data can be obtained free of charge from The Cambridge Crystallographic Data Center via http://www.ccdc.cam.ac.uk/ conts/retrieving.html.

Table S1. Crystal data and structure refinement for [(OEP)Fe(NO)(5-MeIm)]OTf.0.5CH_2Cl_2.

Empirical formula	$(C_{40}H_{50}FeN_7O)(CF_3O_3S)\cdot 0.5(CH_2Cl_2)$	
	$C_{41.5}H_{51}ClF_3FeN_7O_4S$	
Formula weight	892.25	
Crystal system	triclinic	
Space group	$P\bar{1}$	
Unit cell dimensions	a = 8.8510(9) Å	α = 98.2007(15)°
	b = 15.6741(16) Å	β = 105.5290(15)°
	c = 15.9474(16) Å	γ = 93.3465(16)°
Volume	2099.0(4) $Å^3$	
Z, Z'	2, 1	
Density (calculated)	1.412 Mg/m^3	
Wavelength	0.71073 Å	
Temperature	100(2) K	
F(000)	934	
Absorption coefficient	0.537 mm^{-1}	
Absorption correction	semi-empirical from equivalents	
Max. and min. transmission	0.822 and 0.757	
Theta range for data collection	1.319 to 27.497°	
Reflections collected	36273	
Independent reflections	9360 [R(int) = 0.0481]	
Data / restraints / parameters	9360 / 10 / 545	
$wR(F^2$ all data)	$wR2$ = 0.1073	
$R(F$ obsd data)	$R1$ = 0.0383	
Goodness-of-fit on F^2	0.982	
Observed data [I > 2σ(I)]	7918	
Largest and mean shift / s.u.	0.001and 0.000	
Largest diff. peak and hole	0.820 and -0.461 $e/Å^3$	

$wR2 = \{ \Sigma [w(F_o^2 - F_c^2)^2] / \Sigma [w(F_o^2)^2] \}^{1/2}$

$R1 = \Sigma ||F_o| - |F_c|| / \Sigma |F_o|$

Table S2. Atomic coordinates and equivalent isotropic displacement parameters for [(OEP)Fe(NO)(5-MeIm)]OTf.0.5CH_2Cl_2. U(eq) is defined as one third of the trace of the orthogonalized U_{ij} tensor.

	x	y	z	U(eq)
Fe(1)	0.63091(3)	0.75402(2)	0.32947(2)	0.01141(7)
O(1)	0.76783(17)	0.91808(10)	0.32578(12)	0.0372(4)
N(1)	0.49517(16)	0.79818(10)	0.40542(9)	0.0131(3)
N(2)	0.45991(16)	0.76596(10)	0.22086(9)	0.0134(3)
N(3)	0.75893(16)	0.70160(10)	0.25285(9)	0.0132(3)
N(4)	0.79408(16)	0.73312(9)	0.43741(9)	0.0127(3)
N(5)	0.53267(16)	0.63537(10)	0.32267(9)	0.0137(3)
N(6)	0.45115(17)	0.49756(11)	0.27807(10)	0.0165(3)
N(7)	0.71219(16)	0.85141(10)	0.33084(10)	0.0171(3)
C(1)	0.53599(19)	0.81536(11)	0.49601(11)	0.0130(3)
C(2)	0.40910(19)	0.85192(11)	0.52568(11)	0.0137(3)
C(3)	0.28939(19)	0.85399(11)	0.45173(11)	0.0143(3)
C(4)	0.34464(19)	0.82107(11)	0.37707(11)	0.0137(3)
C(5)	0.25950(19)	0.81801(11)	0.29002(11)	0.0145(3)
C(6)	0.31576(19)	0.79594(11)	0.21796(11)	0.0139(3)
C(7)	0.2334(2)	0.80473(11)	0.12848(11)	0.0152(3)
C(8)	0.3312(2)	0.78207(12)	0.07778(11)	0.0155(3)
C(9)	0.47151(19)	0.75662(11)	0.13560(11)	0.0143(3)
C(10)	0.5943(2)	0.72331(12)	0.10815(11)	0.0160(3)
C(11)	0.72538(19)	0.69473(12)	0.16248(11)	0.0143(3)
C(12)	0.8441(2)	0.65098(12)	0.13172(11)	0.0156(3)
C(13)	0.95115(19)	0.63257(12)	0.20439(11)	0.0145(3)
C(14)	0.89805(19)	0.66510(11)	0.27988(11)	0.0138(3)
C(15)	0.97769(19)	0.66204(11)	0.36691(11)	0.0142(3)
C(16)	0.93129(18)	0.69515(11)	0.44007(11)	0.0128(3)
C(17)	1.02147(19)	0.69648(11)	0.53096(11)	0.0139(3)
C(18)	0.93539(19)	0.73429(12)	0.58269(11)	0.0147(3)
C(19)	0.79388(19)	0.75717(11)	0.52395(11)	0.0136(3)
C(20)	0.67489(19)	0.79591(11)	0.55149(11)	0.0139(3)
C(21)	0.4134(2)	0.88263(12)	0.61988(11)	0.0169(3)
C(22)	0.5206(2)	0.96648(13)	0.66150(13)	0.0242(4)
C(23)	0.1329(2)	0.88894(12)	0.44513(12)	0.0171(4)
C(24)	0.1370(2)	0.98378(13)	0.43228(13)	0.0231(4)
C(25)	0.0750(2)	0.83808(13)	0.10054(12)	0.0202(4)
C(26)	0.0865(3)	0.93708(15)	0.11240(17)	0.0393(6)
C(27)	0.3016(2)	0.78089(12)	-0.01954(11)	0.0191(4)

C(28)	0.2233(2)	0.69360(14)	-0.07381(12)	0.0248(4)
C(29)	0.8403(2)	0.62649(13)	0.03643(11)	0.0204(4)
C(30)	0.7304(3)	0.54397(14)	-0.00923(13)	0.0305(5)
C(31)	1.0910(2)	0.58240(12)	0.20668(11)	0.0175(4)
C(32)	1.0450(2)	0.48578(14)	0.19767(16)	0.0328(5)
C(33)	1.1804(2)	0.66380(13)	0.56165(12)	0.0183(4)
C(34)	1.1735(2)	0.57312(14)	0.58510(16)	0.0315(5)
C(35)	0.9756(2)	0.75118(13)	0.68179(11)	0.0187(4)
C(36)	1.0384(2)	0.84506(14)	0.72324(12)	0.0247(4)
C(37)	0.5183(2)	0.56841(12)	0.25903(11)	0.0162(3)
C(38)	0.47191(19)	0.60476(12)	0.38543(11)	0.0152(3)
C(39)	0.4208(2)	0.51922(12)	0.35877(11)	0.0168(4)
C(40)	0.3445(2)	0.45627(13)	0.40086(13)	0.0248(4)
S(1A)	0.45475(5)	0.27161(3)	0.20257(3)	0.01811(11)
O(1A)	0.42523(17)	0.29334(9)	0.28745(9)	0.0258(3)
O(2A)	0.58169(17)	0.21904(10)	0.20060(9)	0.0274(3)
O(3A)	0.44809(17)	0.34391(9)	0.15446(9)	0.0259(3)
C(1A)	0.2797(2)	0.20034(13)	0.13879(13)	0.0235(4)
F(1A)	0.28699(15)	0.17185(9)	0.05671(8)	0.0337(3)
F(2A)	0.14861(14)	0.24012(9)	0.13178(8)	0.0319(3)
F(3A)	0.26346(17)	0.13108(9)	0.17707(9)	0.0411(3)
Cl(1S)	0.4631(2)	1.00628(10)	-0.03532(11)	0.0565(4)
C(2S)	0.5075(6)	1.0135(4)	0.0816(2)	0.0519(15)
Cl(3S)	0.68244(17)	0.96451(10)	0.12239(10)	0.0548(4)

Table S3. Bond lengths [Å] and angles [°] for [(OEP)Fe(NO)(5-MeIm)]OTf.0.5CH_2Cl_2.

Fe(1)-N(7)	1.6437(16)	C(14)-C(15)	1.387(2)
Fe(1)-N(5)	1.9823(15)	C(15)-C(16)	1.381(2)
Fe(1)-N(3)	2.0039(14)	C(15)-H(15)	0.9500
Fe(1)-N(1)	2.0066(14)	C(16)-C(17)	1.452(2)
Fe(1)-N(4)	2.0102(14)	C(17)-C(18)	1.365(2)
Fe(1)-N(2)	2.0119(14)	C(17)-C(33)	1.506(2)
O(1)-N(7)	1.152(2)	C(18)-C(19)	1.447(2)
N(1)-C(4)	1.374(2)	C(18)-C(35)	1.504(2)
N(1)-C(1)	1.374(2)	C(19)-C(20)	1.385(2)
N(2)-C(6)	1.377(2)	C(20)-H(20)	0.9500
N(2)-C(9)	1.379(2)	C(21)-C(22)	1.529(3)
N(3)-C(14)	1.378(2)	C(21)-H(21A)	0.9900
N(3)-C(11)	1.378(2)	C(21)-H(21B)	0.9900
N(4)-C(16)	1.377(2)	C(22)-H(22A)	0.9800
N(4)-C(19)	1.378(2)	C(22)-H(22B)	0.9800
N(5)-C(37)	1.326(2)	C(22)-H(22C)	0.9800
N(5)-C(38)	1.384(2)	C(23)-C(24)	1.529(3)
N(6)-C(37)	1.339(2)	C(23)-H(23A)	0.9900
N(6)-C(39)	1.384(2)	C(23)-H(23B)	0.9900
N(6)-H(6N)	0.84(2)	C(24)-H(24A)	0.9800
C(1)-C(20)	1.388(2)	C(24)-H(24B)	0.9800
C(1)-C(2)	1.448(2)	C(24)-H(24C)	0.9800
C(2)-C(3)	1.364(2)	C(25)-C(26)	1.530(3)
C(2)-C(21)	1.500(2)	C(25)-H(25A)	0.9900
C(3)-C(4)	1.445(2)	C(25)-H(25B)	0.9900
C(3)-C(23)	1.502(2)	C(26)-H(26A)	0.9800
C(4)-C(5)	1.383(2)	C(26)-H(26B)	0.9800
C(5)-C(6)	1.379(2)	C(26)-H(26C)	0.9800
C(5)-H(5)	0.9500	C(27)-C(28)	1.527(3)
C(6)-C(7)	1.448(2)	C(27)-H(27A)	0.9900
C(7)-C(8)	1.362(2)	C(27)-H(27B)	0.9900
C(7)-C(25)	1.502(2)	C(28)-H(28A)	0.9800
C(8)-C(9)	1.450(2)	C(28)-H(28B)	0.9800
C(8)-C(27)	1.500(2)	C(28)-H(28C)	0.9800
C(9)-C(10)	1.379(2)	C(29)-C(30)	1.535(3)
C(10)-C(11)	1.390(2)	C(29)-H(29A)	0.9900
C(10)-H(10)	0.9500	C(29)-H(29B)	0.9900
C(11)-C(12)	1.442(2)	C(30)-H(30A)	0.9800
C(12)-C(13)	1.365(2)	C(30)-H(30B)	0.9800
C(12)-C(29)	1.504(2)	C(30)-H(30C)	0.9800
C(13)-C(14)	1.444(2)	C(31)-C(32)	1.522(3)
C(13)-C(31)	1.500(2)	C(31)-H(31A)	0.9900

C(31)-H(31B)	0.9900	C(38)-C(39)	1.359(3)
C(32)-H(32A)	0.9800	C(38)-H(38)	0.9500
C(32)-H(32B)	0.9800	C(39)-C(40)	1.494(3)
C(32)-H(32C)	0.9800	C(40)-H(40A)	0.9800
C(33)-C(34)	1.522(3)	C(40)-H(40B)	0.9800
C(33)-H(33A)	0.9900	C(40)-H(40C)	0.9800
C(33)-H(33B)	0.9900	S(1A)-O(2A)	1.4359(14)
C(34)-H(34A)	0.9800	S(1A)-O(1A)	1.4439(14)
C(34)-H(34B)	0.9800	S(1A)-O(3A)	1.4518(14)
C(34)-H(34C)	0.9800	S(1A)-C(1A)	1.820(2)
C(35)-C(36)	1.530(3)	C(1A)-F(2A)	1.335(2)
C(35)-H(35A)	0.9900	C(1A)-F(3A)	1.338(2)
C(35)-H(35B)	0.9900	C(1A)-F(1A)	1.341(2)
C(36)-H(36A)	0.9800	Cl(1S)-C(2S)	1.784(4)
C(36)-H(36B)	0.9800	C(2S)-Cl(3S)	1.775(4)
C(36)-H(36C)	0.9800	C(2S)-H(2S1)	0.9900
C(37)-H(37)	0.9500	C(2S)-H(2S2)	0.9900

N(7)-Fe(1)-N(5)	177.65(7)	C(37)-N(5)-C(38)	106.18(15)
N(7)-Fe(1)-N(3)	90.61(7)	C(37)-N(5)-Fe(1)	126.95(12)
N(5)-Fe(1)-N(3)	87.57(6)	C(38)-N(5)-Fe(1)	126.80(12)
N(7)-Fe(1)-N(1)	93.40(7)	C(37)-N(6)-C(39)	108.35(16)
N(5)-Fe(1)-N(1)	88.42(6)	C(37)-N(6)-H(6N)	125.9(15)
N(3)-Fe(1)-N(1)	175.98(6)	C(39)-N(6)-H(6N)	125.6(15)
N(7)-Fe(1)-N(4)	94.38(7)	O(1)-N(7)-Fe(1)	175.38(16)
N(5)-Fe(1)-N(4)	87.11(6)	N(1)-C(1)-C(20)	125.06(15)
N(3)-Fe(1)-N(4)	90.17(6)	N(1)-C(1)-C(2)	110.30(14)
N(1)-Fe(1)-N(4)	89.81(6)	C(20)-C(1)-C(2)	124.55(15)
N(7)-Fe(1)-N(2)	89.91(7)	C(3)-C(2)-C(1)	106.54(15)
N(5)-Fe(1)-N(2)	88.60(6)	C(3)-C(2)-C(21)	127.81(15)
N(3)-Fe(1)-N(2)	89.68(6)	C(1)-C(2)-C(21)	125.64(15)
N(1)-Fe(1)-N(2)	90.05(6)	C(2)-C(3)-C(4)	106.86(14)
N(4)-Fe(1)-N(2)	175.71(6)	C(2)-C(3)-C(23)	128.36(16)
C(4)-N(1)-C(1)	106.05(14)	C(4)-C(3)-C(23)	124.65(15)
C(4)-N(1)-Fe(1)	126.75(11)	N(1)-C(4)-C(5)	125.65(16)
C(1)-N(1)-Fe(1)	127.14(11)	N(1)-C(4)-C(3)	110.23(14)
C(6)-N(2)-C(9)	106.01(13)	C(5)-C(4)-C(3)	124.03(15)
C(6)-N(2)-Fe(1)	126.86(11)	C(6)-C(5)-C(4)	125.20(15)
C(9)-N(2)-Fe(1)	126.64(11)	C(6)-C(5)-H(5)	117.4
C(14)-N(3)-C(11)	106.18(14)	C(4)-C(5)-H(5)	117.4
C(14)-N(3)-Fe(1)	126.92(11)	N(2)-C(6)-C(5)	125.25(15)
C(11)-N(3)-Fe(1)	126.90(11)	N(2)-C(6)-C(7)	110.27(15)
C(16)-N(4)-C(19)	106.17(13)	C(5)-C(6)-C(7)	124.42(15)
C(16)-N(4)-Fe(1)	127.06(11)	C(8)-C(7)-C(6)	106.75(15)
C(19)-N(4)-Fe(1)	126.73(11)	C(8)-C(7)-C(25)	127.88(16)

C(6)-C(7)-C(25)	125.26(16)	H(21A)-C(21)-H(21B)	107.7
C(7)-C(8)-C(9)	106.85(15)	C(21)-C(22)-H(22A)	109.5
C(7)-C(8)-C(27)	127.77(15)	C(21)-C(22)-H(22B)	109.5
C(9)-C(8)-C(27)	125.36(16)	H(22A)-C(22)-H(22B)	109.5
N(2)-C(9)-C(10)	125.10(15)	C(21)-C(22)-H(22C)	109.4
N(2)-C(9)-C(8)	110.08(15)	H(22A)-C(22)-H(22C)	109.5
C(10)-C(9)-C(8)	124.72(16)	H(22B)-C(22)-H(22C)	109.5
C(9)-C(10)-C(11)	125.03(16)	C(3)-C(23)-C(24)	112.20(15)
C(9)-C(10)-H(10)	117.5	C(3)-C(23)-H(23A)	109.2
C(11)-C(10)-H(10)	117.5	C(24)-C(23)-H(23A)	109.2
N(3)-C(11)-C(10)	125.33(15)	C(3)-C(23)-H(23B)	109.2
N(3)-C(11)-C(12)	110.05(14)	C(24)-C(23)-H(23B)	109.2
C(10)-C(11)-C(12)	124.59(15)	H(23A)-C(23)-H(23B)	107.9
C(13)-C(12)-C(11)	106.90(15)	C(23)-C(24)-H(24A)	109.6
C(13)-C(12)-C(29)	128.03(16)	C(23)-C(24)-H(24B)	109.4
C(11)-C(12)-C(29)	124.96(15)	H(24A)-C(24)-H(24B)	109.5
C(12)-C(13)-C(14)	106.87(15)	C(23)-C(24)-H(24C)	109.4
C(12)-C(13)-C(31)	127.43(16)	H(24A)-C(24)-H(24C)	109.5
C(14)-C(13)-C(31)	125.54(15)	H(24B)-C(24)-H(24C)	109.5
N(3)-C(14)-C(15)	125.06(15)	C(7)-C(25)-C(26)	112.38(16)
N(3)-C(14)-C(13)	109.98(14)	C(7)-C(25)-H(25A)	109.1
C(15)-C(14)-C(13)	124.94(15)	C(26)-C(25)-H(25A)	109.1
C(16)-C(15)-C(14)	125.77(15)	C(7)-C(25)-H(25B)	109.1
C(16)-C(15)-H(15)	117.1	C(26)-C(25)-H(25B)	109.1
C(14)-C(15)-H(15)	117.1	H(25A)-C(25)-H(25B)	107.9
N(4)-C(16)-C(15)	124.90(15)	C(25)-C(26)-H(26A)	109.4
N(4)-C(16)-C(17)	110.12(14)	C(25)-C(26)-H(26B)	109.4
C(15)-C(16)-C(17)	124.98(15)	H(26A)-C(26)-H(26B)	109.5
C(18)-C(17)-C(16)	106.65(14)	C(25)-C(26)-H(26C)	109.6
C(18)-C(17)-C(33)	126.94(15)	H(26A)-C(26)-H(26C)	109.5
C(16)-C(17)-C(33)	126.41(15)	H(26B)-C(26)-H(26C)	109.5
C(17)-C(18)-C(19)	106.95(14)	C(8)-C(27)-C(28)	112.45(16)
C(17)-C(18)-C(35)	128.15(15)	C(8)-C(27)-H(27A)	109.1
C(19)-C(18)-C(35)	124.90(15)	C(28)-C(27)-H(27A)	109.1
N(4)-C(19)-C(20)	125.44(15)	C(8)-C(27)-H(27B)	109.1
N(4)-C(19)-C(18)	110.10(14)	C(28)-C(27)-H(27B)	109.1
C(20)-C(19)-C(18)	124.45(15)	H(27A)-C(27)-H(27B)	107.8
C(19)-C(20)-C(1)	125.15(16)	C(27)-C(28)-H(28A)	109.5
C(19)-C(20)-H(20)	117.4	C(27)-C(28)-H(28B)	109.5
C(1)-C(20)-H(20)	117.4	H(28A)-C(28)-H(28B)	109.5
C(2)-C(21)-C(22)	113.67(15)	C(27)-C(28)-H(28C)	109.4
C(2)-C(21)-H(21A)	108.8	H(28A)-C(28)-H(28C)	109.5
C(22)-C(21)-H(21A)	108.8	H(28B)-C(28)-H(28C)	109.5
C(2)-C(21)-H(21B)	108.8	C(12)-C(29)-C(30)	112.65(16)
C(22)-C(21)-H(21B)	108.8	C(12)-C(29)-H(29A)	109.1

C(30)-C(29)-H(29A)	109.1	C(35)-C(36)-H(36A)	109.4
C(12)-C(29)-H(29B)	109.1	C(35)-C(36)-H(36B)	109.5
C(30)-C(29)-H(29B)	109.1	H(36A)-C(36)-H(36B)	109.5
H(29A)-C(29)-H(29B)	107.8	C(35)-C(36)-H(36C)	109.5
C(29)-C(30)-H(30A)	109.5	H(36A)-C(36)-H(36C)	109.5
C(29)-C(30)-H(30B)	109.5	H(36B)-C(36)-H(36C)	109.5
H(30A)-C(30)-H(30B)	109.5	N(5)-C(37)-N(6)	110.50(15)
C(29)-C(30)-H(30C)	109.4	N(5)-C(37)-H(37)	124.7
H(30A)-C(30)-H(30C)	109.5	N(6)-C(37)-H(37)	124.7
H(30B)-C(30)-H(30C)	109.5	C(39)-C(38)-N(5)	109.52(16)
C(13)-C(31)-C(32)	110.93(15)	C(39)-C(38)-H(38)	125.2
C(13)-C(31)-H(31A)	109.5	N(5)-C(38)-H(38)	125.2
C(32)-C(31)-H(31A)	109.5	C(38)-C(39)-N(6)	105.45(16)
C(13)-C(31)-H(31B)	109.5	C(38)-C(39)-C(40)	131.17(17)
C(32)-C(31)-H(31B)	109.5	N(6)-C(39)-C(40)	123.37(17)
H(31A)-C(31)-H(31B)	108.0	C(39)-C(40)-H(40A)	109.4
C(31)-C(32)-H(32A)	109.4	C(39)-C(40)-H(40B)	109.5
C(31)-C(32)-H(32B)	109.5	H(40A)-C(40)-H(40B)	109.5
H(32A)-C(32)-H(32B)	109.5	C(39)-C(40)-H(40C)	109.5
C(31)-C(32)-H(32C)	109.5	H(40A)-C(40)-H(40C)	109.5
H(32A)-C(32)-H(32C)	109.5	H(40B)-C(40)-H(40C)	109.5
H(32B)-C(32)-H(32C)	109.5	O(2A)-S(1A)-O(1A)	115.74(8)
C(17)-C(33)-C(34)	114.06(16)	O(2A)-S(1A)-O(3A)	115.82(9)
C(17)-C(33)-H(33A)	108.7	O(1A)-S(1A)-O(3A)	113.40(9)
C(34)-C(33)-H(33A)	108.7	O(2A)-S(1A)-C(1A)	103.75(9)
C(17)-C(33)-H(33B)	108.7	O(1A)-S(1A)-C(1A)	102.82(9)
C(34)-C(33)-H(33B)	108.7	O(3A)-S(1A)-C(1A)	102.85(9)
H(33A)-C(33)-H(33B)	107.6	F(2A)-C(1A)-F(3A)	107.36(16)
C(33)-C(34)-H(34A)	109.5	F(2A)-C(1A)-F(1A)	107.38(15)
C(33)-C(34)-H(34B)	109.4	F(3A)-C(1A)-F(1A)	107.78(16)
H(34A)-C(34)-H(34B)	109.5	F(2A)-C(1A)-S(1A)	111.89(14)
C(33)-C(34)-H(34C)	109.5	F(3A)-C(1A)-S(1A)	110.70(13)
H(34A)-C(34)-H(34C)	109.5	F(1A)-C(1A)-S(1A)	111.51(14)
H(34B)-C(34)-H(34C)	109.5	Cl(3S)-C(2S)-Cl(1S)	110.2(3)
C(18)-C(35)-C(36)	114.06(15)	Cl(3S)-C(2S)-H(2S1)	109.6
C(18)-C(35)-H(35A)	108.7	Cl(1S)-C(2S)-H(2S1)	109.6
C(36)-C(35)-H(35A)	108.7	Cl(3S)-C(2S)-H(2S2)	109.6
C(18)-C(35)-H(35B)	108.7	Cl(1S)-C(2S)-H(2S2)	109.6
C(36)-C(35)-H(35B)	108.7	H(2S1)-C(2S)-H(2S2)	108.1
H(35A)-C(35)-H(35B)	107.6		

Table S4. Anisotropic displacement parameters ($Å^2 x\ 10^3$) for [(OEP)Fe(NO)(5-MeIm)]OTf.0.5CH_2Cl_2. The anisotropic displacement factor exponent takes the form: $-2\pi^2[\ h^2\ a^{*2}\ U_{11} + ... + 2\ h\ k\ a^*\ b^*\ U_{12}\ ]$

	U_{11}	U_{22}	U_{33}	U_{23}	U_{13}	U_{12}
Fe(1)	10(1)	14(1)	11(1)	4(1)	2(1)	3(1)
O(1)	24(1)	22(1)	64(1)	18(1)	5(1)	-1(1)
N(1)	12(1)	14(1)	14(1)	4(1)	3(1)	4(1)
N(2)	11(1)	16(1)	13(1)	4(1)	2(1)	4(1)
N(3)	11(1)	18(1)	12(1)	4(1)	3(1)	3(1)
N(4)	11(1)	15(1)	13(1)	3(1)	3(1)	4(1)
N(5)	10(1)	17(1)	14(1)	5(1)	2(1)	4(1)
N(6)	16(1)	13(1)	18(1)	2(1)	3(1)	2(1)
N(7)	11(1)	20(1)	20(1)	5(1)	2(1)	5(1)
C(1)	14(1)	12(1)	15(1)	4(1)	5(1)	2(1)
C(2)	14(1)	12(1)	17(1)	4(1)	7(1)	3(1)
C(3)	13(1)	13(1)	18(1)	4(1)	6(1)	2(1)
C(4)	12(1)	11(1)	18(1)	3(1)	4(1)	2(1)
C(5)	10(1)	16(1)	17(1)	2(1)	2(1)	2(1)
C(6)	12(1)	12(1)	16(1)	2(1)	0(1)	2(1)
C(7)	14(1)	13(1)	15(1)	2(1)	-2(1)	1(1)
C(8)	14(1)	14(1)	15(1)	4(1)	-1(1)	2(1)
C(9)	14(1)	14(1)	13(1)	5(1)	1(1)	2(1)
C(10)	16(1)	20(1)	12(1)	6(1)	3(1)	4(1)
C(11)	14(1)	16(1)	14(1)	3(1)	5(1)	1(1)
C(12)	15(1)	18(1)	14(1)	3(1)	4(1)	2(1)
C(13)	12(1)	16(1)	15(1)	2(1)	4(1)	1(1)
C(14)	10(1)	16(1)	16(1)	3(1)	4(1)	1(1)
C(15)	11(1)	16(1)	15(1)	4(1)	3(1)	4(1)
C(16)	10(1)	14(1)	14(1)	4(1)	1(1)	2(1)
C(17)	13(1)	16(1)	12(1)	4(1)	2(1)	2(1)
C(18)	13(1)	16(1)	14(1)	5(1)	2(1)	3(1)
C(19)	14(1)	15(1)	12(1)	4(1)	2(1)	2(1)
C(20)	14(1)	16(1)	12(1)	3(1)	4(1)	2(1)
C(21)	16(1)	20(1)	17(1)	4(1)	8(1)	4(1)
C(22)	26(1)	25(1)	21(1)	-1(1)	7(1)	3(1)
C(23)	14(1)	19(1)	21(1)	4(1)	7(1)	5(1)
C(24)	22(1)	21(1)	31(1)	9(1)	13(1)	10(1)
C(25)	16(1)	22(1)	19(1)	2(1)	-2(1)	6(1)
C(26)	40(1)	25(1)	45(1)	5(1)	-4(1)	15(1)
C(27)	19(1)	23(1)	14(1)	6(1)	0(1)	4(1)

C(28)	26(1)	28(1)	17(1)	1(1)	3(1)	-1(1)
C(29)	20(1)	31(1)	14(1)	6(1)	7(1)	9(1)
C(30)	47(1)	26(1)	17(1)	3(1)	4(1)	7(1)
C(31)	14(1)	24(1)	16(1)	2(1)	5(1)	6(1)
C(32)	20(1)	24(1)	51(1)	7(1)	2(1)	6(1)
C(33)	13(1)	26(1)	16(1)	5(1)	2(1)	6(1)
C(34)	23(1)	29(1)	44(1)	14(1)	6(1)	12(1)
C(35)	19(1)	26(1)	12(1)	6(1)	3(1)	8(1)
C(36)	23(1)	32(1)	17(1)	1(1)	5(1)	0(1)
C(37)	15(1)	19(1)	15(1)	4(1)	3(1)	4(1)
C(38)	15(1)	17(1)	14(1)	4(1)	3(1)	2(1)
C(39)	15(1)	19(1)	16(1)	5(1)	2(1)	4(1)
C(40)	31(1)	22(1)	22(1)	6(1)	8(1)	-2(1)
S(1A)	21(1)	18(1)	16(1)	5(1)	5(1)	5(1)
O(1A)	31(1)	29(1)	17(1)	1(1)	7(1)	7(1)
O(2A)	28(1)	34(1)	26(1)	12(1)	11(1)	15(1)
O(3A)	32(1)	20(1)	26(1)	10(1)	5(1)	3(1)
C(1A)	30(1)	22(1)	19(1)	4(1)	7(1)	2(1)
F(1A)	42(1)	35(1)	20(1)	-6(1)	5(1)	3(1)
F(2A)	22(1)	47(1)	26(1)	7(1)	5(1)	4(1)
F(3A)	52(1)	26(1)	43(1)	14(1)	8(1)	-9(1)
Cl(1S)	74(1)	36(1)	52(1)	2(1)	9(1)	-1(1)
C(2S)	56(3)	56(4)	39(3)	-17(3)	15(2)	21(3)
Cl(3S)	52(1)	48(1)	60(1)	-5(1)	13(1)	14(1)

Table S5. Hydrogen coordinates and isotropic displacement parameters for [(OEP)Fe(NO)(5-MeIm)]OTf.0.5CH_2Cl_2.

	x	y	z	U(eq)
H(6N)	0.437(3)	0.4474(15)	0.2482(14)	0.020
H(5)	0.1539	0.8323	0.2790	0.017
H(10)	0.5888	0.7196	0.0474	0.019
H(15)	1.0725	0.6348	0.3771	0.017
H(20)	0.6895	0.8103	0.6132	0.017
H(21A)	0.4499	0.8367	0.6550	0.020
H(21B)	0.3051	0.8918	0.6228	0.020
H(22A)	0.6305	0.9559	0.6666	0.036
H(22B)	0.5087	0.9865	0.7203	0.036
H(22C)	0.4913	1.0109	0.6243	0.036
H(23A)	0.1021	0.8837	0.4996	0.020
H(23B)	0.0521	0.8537	0.3949	0.020
H(24A)	0.2181	1.0189	0.4814	0.035
H(24B)	0.0340	1.0044	0.4305	0.035
H(24C)	0.1614	0.9888	0.3767	0.035
H(25A)	0.0077	0.8177	0.1357	0.024
H(25B)	0.0238	0.8140	0.0377	0.024
H(26A)	0.1334	0.9612	0.1749	0.059
H(26B)	-0.0192	0.9557	0.0925	0.059
H(26C)	0.1526	0.9578	0.0775	0.059
H(27A)	0.4030	0.7942	-0.0323	0.023
H(27B)	0.2331	0.8267	-0.0375	0.023
H(28A)	0.2925	0.6483	-0.0580	0.037
H(28B)	0.2046	0.6963	-0.1368	0.037
H(28C)	0.1227	0.6802	-0.0615	0.037
H(29A)	0.9483	0.6176	0.0328	0.025
H(29B)	0.8049	0.6749	0.0048	0.025
H(30A)	0.7642	0.4959	0.0220	0.046
H(30B)	0.7343	0.5299	-0.0704	0.046
H(30C)	0.6223	0.5535	-0.0084	0.046
H(31A)	1.1734	0.6024	0.2631	0.021
H(31B)	1.1353	0.5933	0.1579	0.021
H(32A)	1.0055	0.4748	0.2474	0.049
H(32B)	1.1373	0.4542	0.1976	0.049
H(32C)	0.9624	0.4661	0.1422	0.049
H(33A)	1.2449	0.7044	0.6141	0.022
H(33B)	1.2340	0.6639	0.5146	0.022
H(34A)	1.1121	0.5709	0.6277	0.047

H(34B)	1.2807	0.5591	0.6111	0.047
H(34C)	1.1234	0.5311	0.5317	0.047
H(35A)	1.0558	0.7128	0.7055	0.022
H(35B)	0.8801	0.7357	0.6997	0.022
H(36A)	1.1339	0.8608	0.7066	0.037
H(36B)	1.0632	0.8510	0.7876	0.037
H(36C)	0.9582	0.8835	0.7020	0.037
H(37)	0.5509	0.5704	0.2072	0.019
H(38)	0.4668	0.6384	0.4389	0.018
H(40A)	0.4036	0.4054	0.4054	0.037
H(40B)	0.2359	0.4384	0.3648	0.037
H(40C)	0.3442	0.4838	0.4600	0.037
H(2S1)	0.5213	1.0751	0.1095	0.062
H(2S2)	0.4188	0.9840	0.0968	0.062

Table S6. Torsion angles [°] for [(OEP)Fe(NO)(5-MeIm)]OTf.0.5CH_2Cl_2.

C(4)-N(1)-C(1)-C(20)	175.18(16)	C(7)-C(8)-C(9)-C(10)	175.11(17)
Fe(1)-N(1)-C(1)-C(20)	-7.5(3)	C(27)-C(8)-C(9)-C(10)	-3.6(3)
C(4)-N(1)-C(1)-C(2)	-1.30(19)	N(2)-C(9)-C(10)-C(11)	-0.5(3)
Fe(1)-N(1)-C(1)-C(2)	176.04(11)	C(8)-C(9)-C(10)-C(11)	-176.58(17)
N(1)-C(1)-C(2)-C(3)	1.8(2)	C(14)-N(3)-C(11)-C(10)	179.72(17)
C(20)-C(1)-C(2)-C(3)	-174.66(17)	Fe(1)-N(3)-C(11)-C(10)	-0.2(3)
N(1)-C(1)-C(2)-C(21)	-177.03(16)	C(14)-N(3)-C(11)-C(12)	1.45(19)
C(20)-C(1)-C(2)-C(21)	6.5(3)	Fe(1)-N(3)-C(11)-C(12)	-178.49(12)
C(1)-C(2)-C(3)-C(4)	-1.56(19)	C(9)-C(10)-C(11)-N(3)	-5.5(3)
C(21)-C(2)-C(3)-C(4)	177.28(17)	C(9)-C(10)-C(11)-C(12)	172.56(18)
C(1)-C(2)-C(3)-C(23)	-177.49(17)	N(3)-C(11)-C(12)-C(13)	-0.9(2)
C(21)-C(2)-C(3)-C(23)	1.4(3)	C(10)-C(11)-C(12)-C(13)	-179.18(17)
C(1)-N(1)-C(4)-C(5)	177.03(17)	N(3)-C(11)-C(12)-C(29)	175.57(17)
Fe(1)-N(1)-C(4)-C(5)	-0.3(3)	C(10)-C(11)-C(12)-C(29)	-2.7(3)
C(1)-N(1)-C(4)-C(3)	0.31(19)	C(11)-C(12)-C(13)-C(14)	-0.02(19)
Fe(1)-N(1)-C(4)-C(3)	-177.05(11)	C(29)-C(12)-C(13)-C(14)	-176.34(18)
C(2)-C(3)-C(4)-N(1)	0.8(2)	C(11)-C(12)-C(13)-C(31)	175.71(17)
C(23)-C(3)-C(4)-N(1)	176.95(16)	C(29)-C(12)-C(13)-C(31)	-0.6(3)
C(2)-C(3)-C(4)-C(5)	-175.95(17)	C(11)-N(3)-C(14)-C(15)	176.98(17)
C(23)-C(3)-C(4)-C(5)	0.2(3)	Fe(1)-N(3)-C(14)-C(15)	-3.1(3)
N(1)-C(4)-C(5)-C(6)	-3.8(3)	C(11)-N(3)-C(14)-C(13)	-1.46(19)
C(3)-C(4)-C(5)-C(6)	172.51(17)	Fe(1)-N(3)-C(14)-C(13)	178.48(12)
C(9)-N(2)-C(6)-C(5)	-176.79(17)	C(12)-C(13)-C(14)-N(3)	0.9(2)
Fe(1)-N(2)-C(6)-C(5)	-4.4(3)	C(31)-C(13)-C(14)-N(3)	-174.91(16)
C(9)-N(2)-C(6)-C(7)	0.73(19)	C(12)-C(13)-C(14)-C(15)	-177.51(17)
Fe(1)-N(2)-C(6)-C(7)	173.08(11)	C(31)-C(13)-C(14)-C(15)	6.7(3)
C(4)-C(5)-C(6)-N(2)	6.3(3)	N(3)-C(14)-C(15)-C(16)	-0.3(3)
C(4)-C(5)-C(6)-C(7)	-170.88(17)	C(13)-C(14)-C(15)-C(16)	177.89(17)
N(2)-C(6)-C(7)-C(8)	-1.7(2)	C(19)-N(4)-C(16)-C(15)	-179.81(17)
C(5)-C(6)-C(7)-C(8)	175.88(17)	Fe(1)-N(4)-C(16)-C(15)	-2.2(3)
N(2)-C(6)-C(7)-C(25)	-178.18(16)	C(19)-N(4)-C(16)-C(17)	-0.91(19)
C(5)-C(6)-C(7)-C(25)	-0.6(3)	Fe(1)-N(4)-C(16)-C(17)	176.75(11)
C(6)-C(7)-C(8)-C(9)	1.83(19)	C(14)-C(15)-C(16)-N(4)	3.1(3)
C(25)-C(7)-C(8)-C(9)	178.23(17)	C(14)-C(15)-C(16)-C(17)	-175.67(17)
C(6)-C(7)-C(8)-C(27)	-179.49(17)	N(4)-C(16)-C(17)-C(18)	1.1(2)
C(25)-C(7)-C(8)-C(27)	-3.1(3)	C(15)-C(16)-C(17)-C(18)	179.96(17)
C(6)-N(2)-C(9)-C(10)	-176.14(17)	N(4)-C(16)-C(17)-C(33)	-177.96(16)
Fe(1)-N(2)-C(9)-C(10)	11.5(3)	C(15)-C(16)-C(17)-C(33)	0.9(3)
C(6)-N(2)-C(9)-C(8)	0.43(19)	C(16)-C(17)-C(18)-C(19)	-0.74(19)
Fe(1)-N(2)-C(9)-C(8)	-171.94(12)	C(33)-C(17)-C(18)-C(19)	178.27(17)
C(7)-C(8)-C(9)-N(2)	-1.5(2)	C(16)-C(17)-C(18)-C(35)	179.85(17)
C(27)-C(8)-C(9)-N(2)	179.81(16)	C(33)-C(17)-C(18)-C(35)	-1.1(3)

C(16)-N(4)-C(19)-C(20)	-178.28(17)	O(3A)-S(1A)-C(1A)-F(1A)	62.97(15)
Fe(1)-N(4)-C(19)-C(20)	4.0(3)		
C(16)-N(4)-C(19)-C(18)	0.44(19)		
Fe(1)-N(4)-C(19)-C(18)	-177.23(11)		
C(17)-C(18)-C(19)-N(4)	0.2(2)		
C(35)-C(18)-C(19)-N(4)	179.65(16)		
C(17)-C(18)-C(19)-C(20)	178.95(17)		
C(35)-C(18)-C(19)-C(20)	-1.6(3)		
N(4)-C(19)-C(20)-C(1)	1.0(3)		
C(18)-C(19)-C(20)-C(1)	-177.52(17)		
N(1)-C(1)-C(20)-C(19)	0.8(3)		
C(2)-C(1)-C(20)-C(19)	176.76(17)		
C(3)-C(2)-C(21)-C(22)	-107.2(2)		
C(1)-C(2)-C(21)-C(22)	71.4(2)		
C(2)-C(3)-C(23)-C(24)	92.2(2)		
C(4)-C(3)-C(23)-C(24)	-83.0(2)		
C(8)-C(7)-C(25)-C(26)	-91.4(2)		
C(6)-C(7)-C(25)-C(26)	84.4(2)		
C(7)-C(8)-C(27)-C(28)	-90.2(2)		
C(9)-C(8)-C(27)-C(28)	88.3(2)		
C(13)-C(12)-C(29)-C(30)	96.4(2)		
C(11)-C(12)-C(29)-C(30)	-79.3(2)		
C(12)-C(13)-C(31)-C(32)	-86.9(2)		
C(14)-C(13)-C(31)-C(32)	88.0(2)		
C(18)-C(17)-C(33)-C(34)	83.0(2)		
C(16)-C(17)-C(33)-C(34)	-98.2(2)		
C(17)-C(18)-C(35)-C(36)	101.5(2)		
C(19)-C(18)-C(35)-C(36)	-77.9(2)		
C(38)-N(5)-C(37)-N(6)	0.30(18)		
Fe(1)-N(5)-C(37)-N(6)	177.60(11)		
C(39)-N(6)-C(37)-N(5)	-0.33(19)		
C(37)-N(5)-C(38)-C(39)	-0.17(18)		
Fe(1)-N(5)-C(38)-C(39)	-177.47(11)		
N(5)-C(38)-C(39)-N(6)	-0.03(18)		
N(5)-C(38)-C(39)-C(40)	-179.11(17)		
C(37)-N(6)-C(39)-C(38)	0.21(19)		
C(37)-N(6)-C(39)-C(40)	179.39(16)		
O(2A)-S(1A)-C(1A)-F(2A)	-178.37(12)		
O(1A)-S(1A)-C(1A)-F(2A)	60.69(15)		
O(3A)-S(1A)-C(1A)-F(2A)	-57.33(15)		
O(2A)-S(1A)-C(1A)-F(3A)	61.91(16)		
O(1A)-S(1A)-C(1A)-F(3A)	-59.03(16)		
O(3A)-S(1A)-C(1A)-F(3A)	-177.04(14)		
O(2A)-S(1A)-C(1A)-F(1A)	-58.08(15)		
O(1A)-S(1A)-C(1A)-F(1A)	-179.02(13)		

Table S7. Hydrogen bonds for [(OEP)Fe(NO)(5-MeIm)]OTf.0.5CH_2Cl_2 [Å and °].

D-H...A	d(D-H)	d(H...A)	d(D...A)	<(DHA)
N(6)-H(6N)...O(1A)	0.84(2)	2.58(2)	3.224(2)	133.8(18)
N(6)-H(6N)...O(3A)	0.84(2)	2.07(2)	2.880(2)	161(2)
C(40)-H(40A)...O(1A)	0.98	2.44	3.145(3)	128.6
C(2S)-H(2S1)...O(2A)#1	0.99	2.45	3.429(6)	170.4

Symmetry transformations used to generate equivalent atoms:
#1 x, y+1, z

Computational Details

All calculations were done using the program Gaussian 09.[1] Full geometry optimization were conducted for all studied chemical species with subsequent frequency calculations to verify the nature of the corresponding stationary states on their potential energy surfaces and provide zero-point energy corrected electronic energies, enthalpies, and Gibbs free energies.

In the section of computational investigation of ^{1}H NMR shifts and NO vibrational frequencies, geometries were optimized using the mPW1PW91[2] method and the NMR properties were calculated using the B3LYP[3] method with solvent effect included using the PCM formalism,[4-7] similar to the approach used previously to study ^{1}H NMR shifts in various organometallic complexes.[8] The basis set used in the geometry optimization is Wachters' basis[9] for iron, 6-311++G(2d,2p) for 1st shell atoms (atoms bonded to iron, HNO, and BH_3), and 6-31G(d) for other atoms. The basis set used in the NMR calculation is similar with the only difference of using LanL2DZ[10] basis for Fe. The calculated NO frequencies of various iron porphyrin systems studied in this work were scaled using the experimental/computational NO frequency (1380/1568) for a related HNO Ru porphyrin system.[11]

In the section of reaction pathway calculations, three sets of methods were used together with the above geometry optimization basis set. In the first two sets of calculations, the hybrid HF-DFT method mPW1PW91[2] and the pure DFT method mPWVWN[2,12] were used in full geometry optimization and frequency analysis with the experimental chloroform solvent effect included using the PCM formalism.[4-7] For the third set of calculations, the dispersion effect corrected B3LYP-D3[13] method was used to perform single point energy calculations of the mPWVWN optimized structures and generated corrected energy results.

As shown in Table S8 for mPW1PW91 energy results, and Tables S9 and S10 for mPWVWN and B3LYP-D3 energy data, the trends obtained for N- and O-pathways are basically the same, with the formation of HNO complex being of lower Gibbs free energies of activation by ~16-19 kcal/mol and lower Gibbs free reaction energy by ~17-20 kcal/mol than the formation of NOH complex. So, the discussion was focused on the mPW1PW91 data with its geometric and charge results shown in Tables S11 and S12, respectively.

Since for the O-pathway product there could be additional conformations with H in NOH pointing to or away from porphyrin ring and with NO *cis* or *trans* to the Me group in the axial ligand, we studied these different conformations to use the lowest energy one to compare with the N-pathway product formation. The Fe^{II}(Por)(5-MeIm)(NOH_{Down}) structure is more stable than the Fe^{II}(Por)(5-MeIm)(NOH_{up}) (Figure S7) conformation by 3.76 kcal/mol in Gibbs free energy, which is in good agreement with previous computational investigation of these two conformations.[14] However, this Fe^{II}(Por)(5-MeIm)(NOH_{Down}) with a *trans* NO/Me orientation is slightly less stable than a conformation with the *cis* NO/Me orientation by 0.31 kcal/mol. Therefore, the *cis* conformation was used as the lowest energy conformation for the NOH product (**P-1$_O$**).

Scheme S1. DFT-calculated N- and O-pathways for hydride addition to the [(P)Fe(NO)(5-MeIm)]$^{+}$ cation.

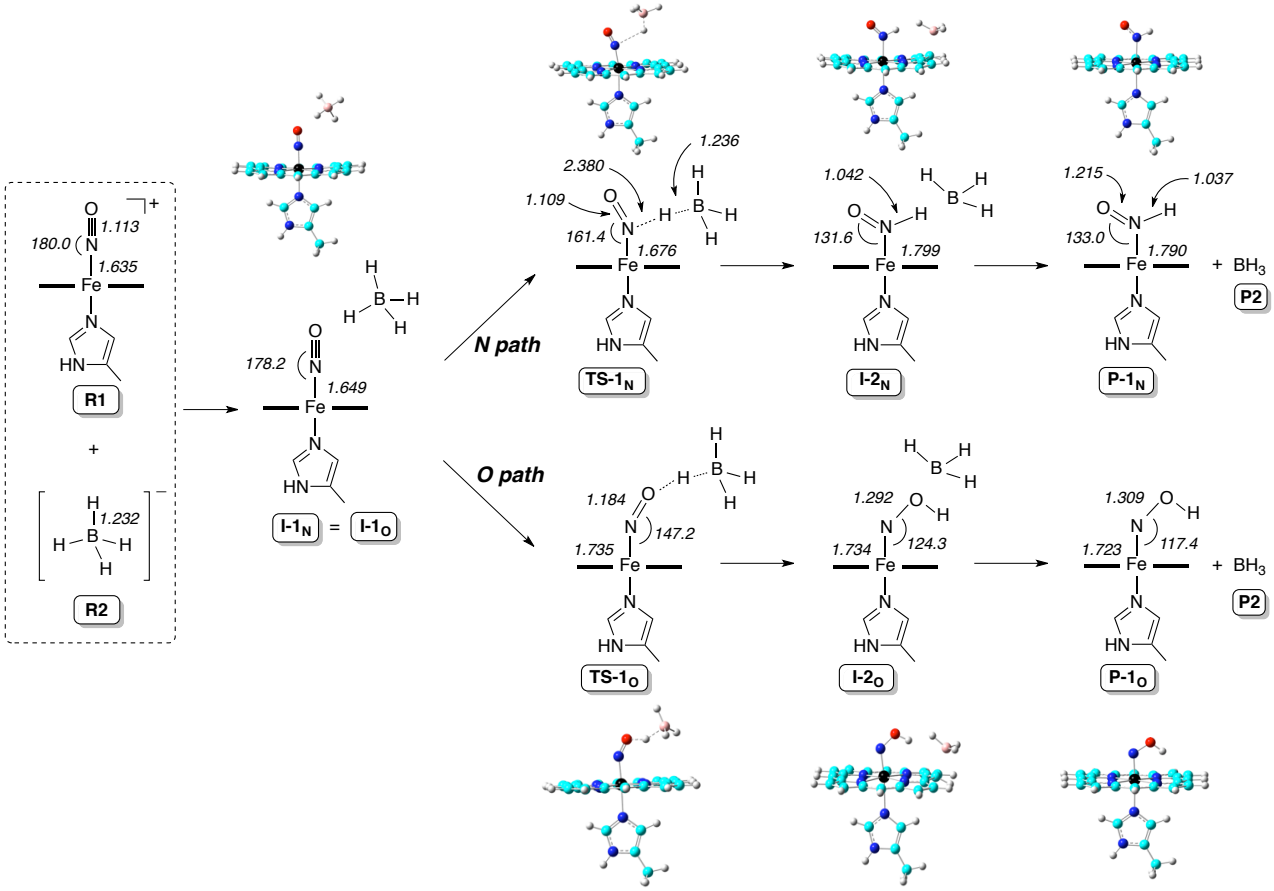

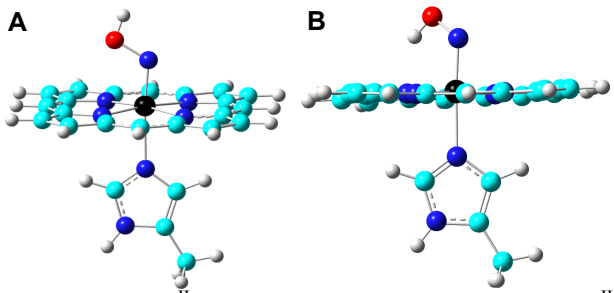

Figure S7. Optimized structures of (A) Fe^{II}(Por)(5-MeIm)(NOH_{up}) and (B) Fe^{II}(Por)(5-MeIm)(NOH_{down}).

Table S8. Relative Energies of All Species in the N- and O-pathways from mPW1PW91 (Units: kcal/mol)

Pathway	System	ΔE_{SCF}	$\Delta E_{SCF+ZPE}$	ΔH	ΔG
	R1+R2	0.00	0.00	0.00	0.00
	I-1$_{N/O}$	-9.81	-8.43	-8.21	0.51
N-Pathway	**TS-1$_N$**	-9.22	-8.10	-8.51	2.25
	I-2$_N$	-41.91	-38.14	-38.76	-27.20
	P-1$_N$ + P2	-29.93	-29.13	-28.76	-28.79
O-Pathway	**TS-1$_O$**	10.47	8.57	8.41	18.59
	I-2$_O$	-18.22	-15.09	-15.62	-4.42
	P-1$_O$ + P2	-8.30	-8.07	-7.57	-8.48

Table S9. Relative Energies of All Species in the N- and O-pathways from mPWVWN calculations (Unit: kcal/mol)

Pathway	System	ΔE_{SCF}	$\Delta E_{SCF+ZPE}$	ΔH	ΔG
	R1+R2	0.00	0.00	0.00	0.00
	I-1$_{N/O}$	-8.36	-7.33	-6.90	0.66
N-Pathway	**TS-1$_N$**	-5.39	-5.40	-5.74	4.33
	I-2$_N$	-18.21	-16.90	-15.77	-11.21
	P-1$_N$ + P2	-17.05	-16.18	-15.85	-15.96
O-Pathway	**TS-1$_O$**	14.64	12.55	12.52	22.26
	I-2$_O$	0.40	2.72	2.53	12.45
	P-1$_O$ + P2	1.30	1.28	1.79	0.72

Table S10. Relative Energies of All Species in the N- and O-pathways from B3LYP-D3 calculations (Unit: kcal/mol)

Pathway	System	ΔE_{SCF}	$\Delta E_{SCF+ZPE}$	ΔH	ΔG
	R1+R2	0.00	0.00	0.00	0.00
	I-1$_{N/O}$	-9.65	-8.62	-8.18	-0.63
N-Pathway	**TS-1$_N$**	-14.16	-13.98	-14.32	-4.25
	I-2$_N$	-31.81	-30.50	-29.37	-24.81
	P-1$_N$ + P2	-29.77	-28.90	-28.57	-28.69
O-Pathway	**TS-1$_O$**	6.88	4.79	4.76	14.50
	I-2$_O$	-18.67	-16.35	-16.54	-6.61
	P-1$_O$ + P2	-8.36	-8.38	-7.88	-8.94

Table S11. Key Geometry Parameters from mPW1PW91 Calculations [a]

Compound	$R_{FeN(L)}$ (Å)	$R_{FeN(NO)}$ (Å)	$R_{B\text{-}N/O}$ (Å)	R_{NO} (Å)	$R_{N/O\text{-}H}$ (Å)	R_{BH} (Å)	∠HNO/ NOH (°)	∠FeNO (°)	∠NFeN(L) (°)
R_1	1.984	1.635		1.113				180.0	179.8
R_2						1.232			
I-$1_{N/O}$	1.987	1.649	3.029	1.106	2.738	1.232	114.6	178.2	179.0
TS-1_N	1.984	1.676	3.116	1.109	2.380	1.236	91.8	161.4	171.1
I-2_N	2.048	1.799	3.752	1.213	1.042	2.795	112.5	131.6	177.8
P-1_N	2.050	1.790		1.215	1.037		112.0	133.0	177.7
TS-1_O	2.029	1.735	2.636	1.184	1.251	1.483	118.7	147.2	177.2
I-2_O	2.106	1.734	3.477	1.292	0.988	2.515	113.9	124.3	174.4
P-1_O	2.115	1.723		1.309	0.977		106.0	117.4	176.0

[a] L is axial ligand

Table S12. NPA Charges from mPW1PW91 Calculations (Unit: e)

	Q_{Fe}	$Q_{N(L)}$	Q_B	Q_H	Q_N	Q_O	$Q_{N(Por)}$
R1	-0.005	-0.414			0.705	-0.040	-0.454
R2			-0.713	-0.072			
I-$1_{N/O}$	0.001	-0.416	-0.713	-0.071	0.700	0.021	-0.457
TS-1_N	0.055	-0.416	-0.671	-0.073	0.686	-0.011	-0.461
I-2_N	0.169	-0.458	-0.205	0.347	0.140	-0.328	-0.458
P-1_N	0.169	-0.453		0.314	0.157	-0.341	-0.468
TS-1_O	0.094	-0.439	-0.237	0.243	0.368	-0.202	-0.464
I-2_O	0.152	-0.476	-0.215	0.496	0.145	-0.469	-0.457
P-1_O	0.140	-0.474		0.482	0.144	-0.472	-0.467
P2			0.331				

References

1. Frisch, M. J.; Trucks, G. W.; Schlegel, H. B.; Scuseria, G. E.; Robb, M. A.; Cheeseman, J. R.; Scalmani, G.; Barone, V.; Mennucci, B.; Petersson, G. A.; Nakatsuji, H.; Caricato, M.; Li, X.; Hratchian, H. P.; Izmaylov, A. F.; Bloino, J.; Zheng, G.; Sonnenberg, J. L.; Hada, M.; Ehara, M.; Toyota, K.; Fukuda, R.; Hasegawa, J.; Ishida, M.; Nakajima, T.; Honda, Y.; Kitao, O.; Nakai, H.; Vreven, T.; Montgomery, Jr., J. A.; J. Peralta, E.; Ogliaro, F.; Bearpark, M.; Heyd, J. J.; Brothers, E.; Kudin, K. N.; Staroverov, V. N.; Keith, T.; Kobayashi, R.; Normand,J.; Raghavachari, K.; Rendell, A.; Burant, J. C.; Iyengar, S. S.; Tomasi, J.; Cossi, M.; Rega, N.; Millam, J. M.; Klene, M.; Knox, J. E.; Cross, J. B.; Bakken, V.; Adamo, C.; Jaramillo, J.; Gomperts, R.; Stratmann, R. E.; Yazyev, O.; Austin, A. J.; Cammi, R.; Pomelli, C.; Ochterski, J. W.; Martin, R. L.; Morokuma, K.; Zakrzewski,V. G.; Voth, G. A.; Salvador, P.; Dannenberg, J. J.; Dapprich, S.; Daniels, A. D.; Farkas, O.; Foresman, J. B.; Ortiz, J. V.; Cioslowski, J.; Fox, D. J.; Gaussian 09, Revision B.01; Gaussian, Inc.: Wallingford CT, 2010.
2. Adamo, C.; Barone, V. *J. Chem. Phys.* 1**998**, *108*, 664-675.
3. Becke, A. D. *J. Chem. Phys.* **1993**, *98*, 5648-5652.

4. Cossi, M.; Barone, V.; Cammi, R.; Tomasi, J. *Chem. Phys. Lett.* **1996**, *255*, 327-335.
5. Mennucci, B.; Tomasi, J. *J. Chem. Phys.* **1997**, *106*, 5151-5158.
6. Cossi, M.; Barone, V.; Mennucci, B.; Tomasi, J. *Chem. Phys. Lett.* **1998**, *286*, 253-260.
7. Cossi, M.; Scalmani, G.; Rega, N.; Barone, V. *J. Chem. Phys.* **2002**, *117*, 43-54.
8. Zhang, Y.; Lewis, J. C.; Bergman, R. G.; Ellman, J. A.; Oldfield, E. *Organometallics* **2006**, *25*, 3515-3519.
9. Wachters, A. J. *J. Chem. Phys.* **1970**, *52*, 1033-1036.
10. Hay, P. J.; Wadt, W. R. *J. Chem. Phys.* **1985**, *82*, 270-283.
11. Lee, J. Y.; Richter-Addo, G. B. *J. Inorg. Biochem.* **2004**, *98*, 1247-1250.
12. Vosko, S. H.; Wilk, L.; Nusair, M. *Can. J. Phys.* **1980**, *58*, 1200-1211.
13. Grimme, S.; Antony, J.; Ehrlich, S.; Krieg, H. *J. Chem. Phys.* **2010**, *132*, 154104.
14. Linder, D. P.; Rodgers, K. R. *Inorg. Chem.* **2005**, *44*, 8259-8264.